ministerie van verkeer en waterstaat

koninklijk nederlands meteorologisch instituut

GCM control run of UK Meteorological Office compared with the real climate in the NW European winter

J.J. Beersma

Scientific reports ; WR 92 - 02
Wetenschappelijke rapporten; WR 92 - 02

De Bilt, 1992

De Bilt 1992

publicationnumber: Scientific reports =
Wetenschappelijke rapporten;
WR 92-02

p.o. box 201
3730 AE De Bilt
Wilhelminalaan 10
tel.+31 30 206 911
telex 470 96

Department of Physical Meteorology

UDC: "324" 551.509.3 551.577.3
551.513.1 551.524.3 (4-16)

ISSN: 0169-1651

ISBN: 90-369-2021-3

GCM control run of UK Meteorological Office compared with the real climate in the NW European winter

J.J. Beersma

June 1992

KNMI Afdeling Fysische Meteorologie
Werkgroep Klimaatscenario's

Abstract

A method is presented to compare the statistical properties of surface air temperature, sea surface temperature, precipitation, global radiation, 500 mbar height, sea level pressure, and wind generated by a GCM with those of observations. As an illustration the control run of a UKMO 11-layer GCM for five successive winters (DJF) is compared with observations for NW Europe. In this comparison large differences are found in (monthly) mean values, standard deviations and autocorrelation coefficients for various elements.

In general, this GCM winter run creates too low temperatures over land, too high temperatures over sea, large temperature variability but small pressure variability and too small autocorrelation coefficients for time-lags of more than three days. Too many wet days are created with too little precipitation. The 500 mbar circulation is veered with respect to reality and shows a peculiar trough over the North Sea. The wind at 100 m is backed and the geostrophic wind is somewhat underestimated. No physically realistic transition of the surface temperature from land to sea is observed.

These results suggest that care has to be taken in interpreting direct model output on a regional scale such as NW Europe. Given the limitations of this study, the relatively short GCM run and difficulties related to comparing GCM grid points with station observations, further work along these lines is desirable, preferably on the basis of the output of more recent GCM versions.

Contents

1 Introduction 3

2 Model description 4

3 Surface air temperature 5
- 3.1 Average surface air temperature 5
- 3.2 Average air temperature as function of height 6
- 3.3 Standard deviation of monthly and daily means 7
- 3.4 Autocorrelation 9

4 Sea surface temperature 11
- 4.1 Average sea surface temperature 11
- 4.2 Standard deviation of monthly means 11

5 Precipitation 12
- 5.1 Average monthly precipitation 12
- 5.2 Average number of days with precipitation 12
- 5.3 Large scale rain, convective rain and snowfall 14

6 Global radiation 15
- 6.1 Average monthly global radiation 15
- 6.2 Standard deviation of monthly total 15

7 500 mbar circulation 16

8 Sea level pressure 19
- 8.1 Mean sea level pressure 19
- 8.2 Standard deviation of monthly and daily means 22
- 8.3 Autocorrelation 23

9 Wind 24
- 9.1 Average 100 m wind speed and average geostrophic wind speed 24
- 9.2 Wind distribution 25

10 Discussion and conclusions 27

Acknowledgement 28

Appendix 29

References 31

1. Introduction

This paper presents a comparison of climate and climate variability simulated by a UKMO (United Kingdom Meteorological Office) 11-layer AGCM (Atmospheric General Circulation Model) [1] with observations for a part of Western Europe. Reference is made to Wilson and Mitchell's comments [2] regarding the importance of studying the higher order moments of climate variable statistics, and of carefully verifying the models' ability to reproduce observed variability on regional scales.

This study therefore not only considers the (time averaged) *mean* of climate variables but also the *standard deviation* and *autocorrelation coefficients* where available. The study area consists of 9 grid points close to the Netherlands. Three grid points are defined by the model as sea points and the remaining six are defined as land points. A map of this area including the locations of the grid points is given in Figure 1. The grid points are compared with single station observations where the selected stations are chosen as close to the grid points as possible.

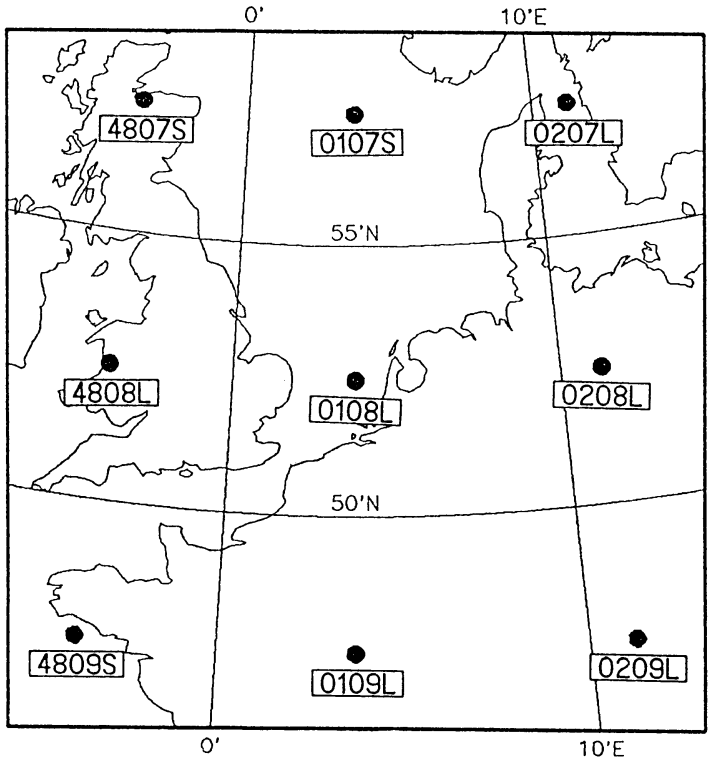

Figure 1. *Map of the study area with the locations of the GCM grid points* L: *Land grid point,* S: *Sea grid point.*

The analyzed GCM control run output consists of five successive winters (DJF), therefore the validation is restricted to the winter. The climate

variables that are discussed in the following sections are: surface air temperature, sea surface temperature, precipitation, global radiation, 500 mbar circulation, sea level pressure and wind. It is emphasized, that the present study focuses on the methodology of comparison rather than on the skill of the specific GCM used here.

2. Model description

The United Kingdom Meteorological Office Model [3] used has a regular latitude-longitude grid with a horizontal resolution of $5° \times 7.5°$. The primitive equations are solved using finite differences on 11 sigma layers which are irregularly spaced, giving enhanced resolution in the boundary layer and near the tropopause.

The model years are made up of twelve months each of 30 days. The small error thus introduced into the incoming solar radiation is minimized by a slight adjustment to the date of perihelion. Seasonal and diurnal variations of solar radiation are incorporated.

The ocean is represented by a 50 m slab in which the heat convergence due to oceanic dynamics is prescribed.

The treatment of the boundary layer uses the Richards scheme. The boundary layer is allowed to occupy up to three of the lowest model layers, with the top being diagnosed at the position of the lowest inversion.

Convection is modeled by a penetrative scheme, which allows entrainment of environmental air and detrainment from the convective parcel at each level. Supersaturation produced by large-scale ascent or following convection is removed by condensation to form precipitation.

Clouds are represented by an interactive cloud scheme which allows for three layer clouds and a convective tower. The layer clouds are assumed to be one sigma layer in thickness, but the convective cloud may occupy more than one sigma layer. Radiative cloud properties are fixed.

The surface albedo varies geographically over land and increases with snow depth over snow covered land but is prescribed over unfrozen sea and land ice.

3. Surface air temperature

3.1 Average surface air temperature

The model daily mean surface temperature is according to Wilson and Mitchell [2] similar to the temperature at the ground. For comparison daily mean screen temperatures from climatological stations are used. As a result of the heating of the surface the maximum diurnal variation occurs at the soil surface and decreases with increasing height. Parton and Logan [4] used data which shows that the daily averaged temperature for both January and July is almost independent of height between 10 cm and 150 cm above the surface. Differences between surface and screen temperatures can therefore be neglected.

TABLE 1. *Average surface air temperature* (°C)

GRID	Land Sea	DEC		JAN		FEB	
		GCM	Obs.	GCM	Obs.	GCM	Obs.
4807[1]	S	10.7	3.8	9.4	2.6	8.7	2.9
0107[2]	S	9.0	-	7.7	-	6.7*	4.6
0207[3]	L	-11.0	1.8	-11.6	-0.3	-9.9	-1.6
4808[4]	L	-5.7	4.4	-2.5	3.7	0.8*	4.0
0108[5]	L	-9.9*	3.2	-5.3	2.0	-4.4*	2.3
0208[6]	L	-12.1	1.3	-8.2	-0.4	-7.2	0.0
4809[7]	S	13.6	8.2	12.4	7.0	12.3	6.8
0109[8]	L	-4.0	3.6	1.9	2.8	3.3	3.6
0209[9]	L	-8.4	-0.8	-4.3	-2.4	-2.7	-1.1

Obs. [1]*Aberdeen (GB), 1931-60* [5]; [2]*North Sea, 1961-80* [6];
[3]*Skagen (DK), 1931-60* [7]; [4]*Central England, 1881-1960* [8,Vol.5];
[5]*De Bilt (NL), 1951-80* [9]; [6]*Lüchow (D), 1931-60* [7];
[7]*Belle-Île (F), 1931-60* [5]; [8]*Nevers (F), 1931-60* [7];
[9]*Bad Tölz (D), 1931-60* [7].
**Student's t-test is applied.*

The average surface air temperatures are shown in Table 1. The GCM control run underestimates the surface air temperature of the land points by 1-13°C but the surface air temperature of the sea points on the other hand is overestimated by 2-7°C. So there is a remarkably strong temperature gradient from land to sea in the GCM.

The differences between the observed surface air temperatures and the values from the GCM simulation in Table 1 are in most cases much larger than the standard deviations of the monthly air temperatures (these are presented in Table 2 of section 3.3). This suggests that these differences are statistically significant. In the cases where the observed and simulated temperatures have the same standard deviation (according to the F-statistic)

this is confirmed by Student's t-test. In all 4 cases where this test can be applied the difference in average air temperature is significant at the 1%-level.

Figure 2 gives plots of the average winter (DJF) surface air temperature calculated with 25 instead of 9 GCM grid points compared with a 10-year mean ECMWF (European Centre for Medium Range Weather Forecasts) analysis projected onto the model grid.

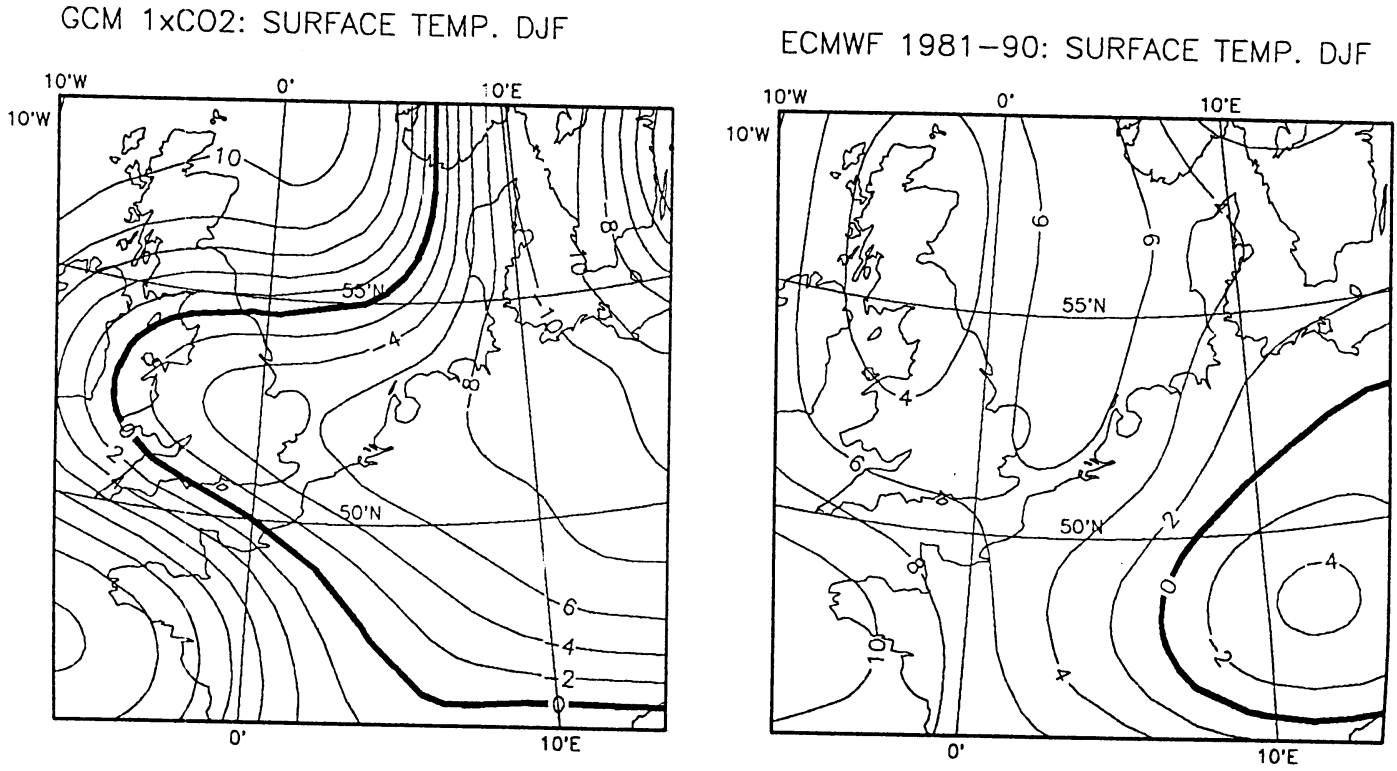

Figure 2. *Average winter (DJF) surface air temperature.*

3.2 Average air temperature as function of height

From the temperature-height (HT) diagram for the grid points 0107 and 0108 in Figure 3 it is seen that the strong temperature gradient between land and sea vanishes at higher model levels. The average winter temperature over sea is at levels higher than 750 mbar about 2°C lower than over land. The air is unstable if the temperature decrease with height is larger than that of the corresponding dry adiabatic. Saturated adiabatics indicate neutral (wet) stability. If the decrease of temperature with height is less than that of the corresponding saturated adiabatic or if the temperature increases with height the air is stable. The air is called conditionally unstable if the slope of the HT-curve is between those of the dry and the saturated

adiabatic. During winter the atmosphere is on average very stable over land (grid point 0108) up to about 850 mbar where it becomes approximately neutral. Over sea (grid point 0107) the atmosphere is approximately neutral except for the surface layer which is very unstable.

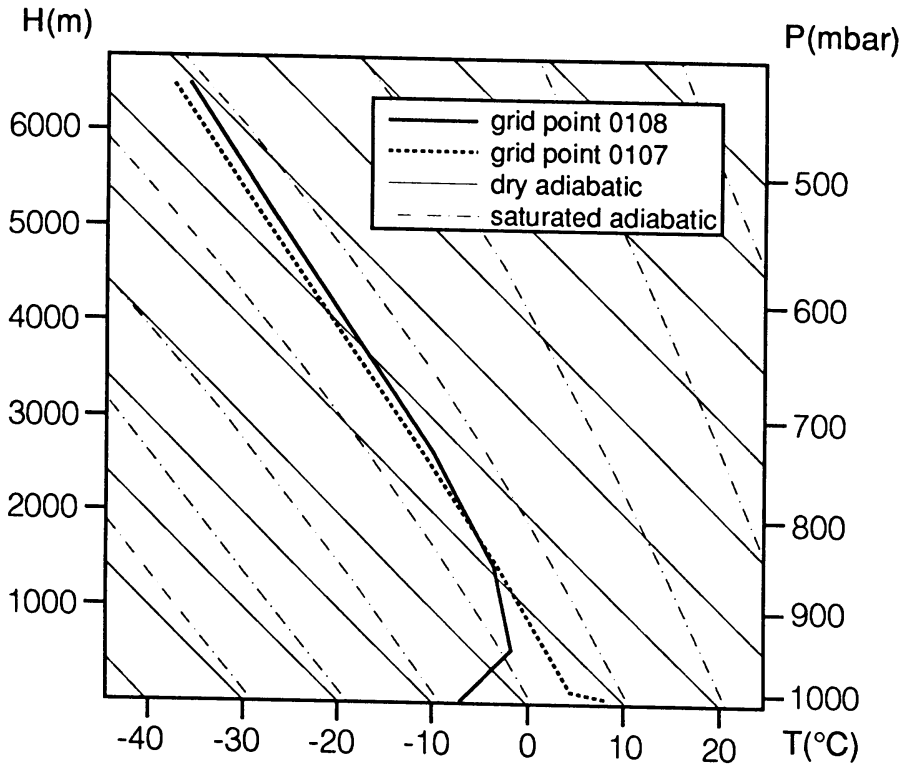

Figure 3. *Average midnight winter temperature as function of height (HT diagram).*

3.3 Standard deviation of monthly and daily means

Table 2 shows the standard deviation of the monthly mean surface temperatures. In most cases standard deviations in the GCM control run for land points are larger than those of the observed series. For Central England the difference becomes statistically significant at the 5%-level (using an F-test) in December. The January difference is both for Central England and De Bilt (NL) even significant at the 1%-level. At sea (the North Sea) only one observed standard deviation of the monthly surface temperature was available being not significantly larger than the value generated by the GCM.

TABLE 2. *Standard deviation of monthly mean surface temperatures* (°C)

GRID	Land Sea	DEC GCM	DEC Obs.	JAN GCM	JAN Obs.	FEB GCM	FEB Obs.
4807	S	0.8	-	0.9	-	0.9	-
0107[2]	S	1.2	-	1.0	-	0.9	1.4
0207	L	4.0	-	3.7	-	4.2	-
4808[4]	L	3.4®	1.7	6.7†	1.8	2.7	1.9
0108[5]	L	2.9	2.1	5.0†	2.3	2.5	2.6
0208	L	1.9	-	4.5	-	2.2	-
4809	S	1.1	-	1.4	-	1.2	-
0109	L	4.9	-	3.3	-	0.2	-
0209	L	2.1	-	3.1	-	2.0	-

Obs. [2]*North Sea, 1961-80* [6]; [5]*De Bilt (NL), 1951-80* [9];
[4]*Central England, 1881-1960* [8,Vol.5].
†(®)*Standard deviations significantly different at the 1% (5%) - level according to the F-test.*

Observed standard deviations of the daily mean surface temperature were only available for De Bilt (NL) and are presented in Table 3. The standard deviations of the daily mean surface temperature are overestimated by about 50% in the GCM control simulation. A similar overestimation of daily temperature variability in GCM experiments is found by Mearns *et al.* [10].

TABLE 3. *Standard deviation of daily mean surface temperatures* (°C)

GRID	Land Sea	DEC GCM	DEC Obs.	JAN GCM	JAN Obs.	FEB GCM	FEB Obs.
0108[5]	L	6.3†	4.1	6.9	4.2	6.4♯	4.1

Obs. [5]*De Bilt (NL), 1951-80*
†(♯)*Standard deviations significantly different at the 1% (10%) - level.*

The significance of differences in daily variability can not easily be tested because atmospheric time series are autocorrelated. A significance test for differences in daily variability is proposed by Katz [11]. His method requires that an autoregressive process is fitted to the data. This autoregressive process is used to obtain residuals that are approximately uncorrelated ('prewhitening'). A test of significance is then applied to the the variances of the residuals (innovation variances). A slight modification of the method proposed by Katz which avoids the use of zero starting values is outlined in the Appendix. Applying this modified method with a second order autoregressive process to the daily mean surface temperatures of Table 3 results in significant differences between observed and simulated daily variance for December (at the 1% - level) and February (at the

10 % - level).

Spatial averaging generally reduces the standard deviation. The reduction in standard deviation is relatively small when an element has strong spatial correlation. This situation applies to temperature if considered on the scale of a grid box. Hence the daily mean temperature standard deviation of the observed climate would be only moderately reduced if in Table 3 grid box averages had been considered rather than point observations.

3.4 Autocorrelation

A comparison of the autocorrelation coefficients of the GCM control run for grid point 0108 with those of the observed data at De Bilt (NL) is presented in Table 4. The lag k autocorrelation coefficient indicates the dependency of one day's temperature and the temperature k days earlier. The standard errors of the autocorrelation coefficients are calculated with the jackknife [12]. In the jackknife method the required statistic is recomputed a large number of times after successive deletion of a group of observations from the entire data set. For example, for the GCM data set which consists of 5 years, the autocorrelation coefficients are calculated 5 times, each time omitting a different year. From the resulting 5 autocorrelation coefficients the standard error is calculated.

TABLE 4. *Autocorrelation coefficients of daily air temperature*

	DEC		JAN		FEB	
LAG	GCM	Obs.	GCM	Obs.	GCM	Obs.
1	0.80±0.02	0.78±0.02	0.86±0.05	0.79±0.03	0.88±0.02	0.83±0.02
2	0.46±0.05	0.53±0.04	0.69±0.08	0.60±0.04	0.69±0.05	0.66±0.05
3	0.17±0.09	0.39±0.06	0.55±0.10	0.48±0.05	0.50±0.08	0.54±0.06
4	0.00±0.10	0.29±0.06	0.45±0.14	0.39±0.06	0.32±0.10	0.46±0.08
5	0.02±0.08	0.23±0.06	0.41±0.17	0.32±0.07	0.19±0.11	0.39±0.09
6	0.04±0.06	0.20±0.06	0.36±0.20	0.25±0.08	0.07±0.11	0.32±0.10
7	0.09±0.11	0.16±0.06	0.31±0.22	0.20±0.09	-0.03±0.12	0.26±0.10
8	0.11±0.17	0.14±0.06	0.25±0.23	0.18±0.09	-0.08±0.11	0.22±0.11
9	0.09±0.17	0.13±0.06	0.21±0.24	0.15±0.10	-0.11±0.11	0.19±0.11
10	0.06±0.14	0.11±0.06	0.18±0.24	0.12±0.10	-0.11±0.12	0.16±0.10

GCM *GCM control run results of grid point 0108*
Obs. *Observations from De Bilt (NL) period 1951-80*
The standard errors of the autocorrelation coefficients are calculated with the Jackknife [12].

The variance of the autocorrelation coefficients of a stationary linear process can also be approximated with Bartlett's formula [13]. According to this formula the standard errors of the first-order autocorrelation

coefficients of the GCM control run are about 0.03 and those of the observed data about 0.02 assuming a second order autoregressive process. The standard errors of the first-order autocorrelation coefficients calculated with the jackknife are of the same order. The first-order autocorrelation coefficients do not differ significantly. For increasing lag both December and February show a rapid decrease of autocorrelation coefficients in the GCM control simulation. On the other hand, for January the autocorrelation coefficients of the GCM experiment and observed data have similar decrease rates. For this month the higher order GCM autocorrelation coefficients even exceed the observed ones. The reason for these high autocorrelation coefficients (with large standard errors) is that the GCM generated for January year 5 a persisting situation which was very cold compared with the other years. This anomalous January situation also leads to a high value of the standard deviation of the monthly mean for January (Table 2).

Because of the high standard errors it is difficult to distinguish systematic differences in autocorrelation between the GCM control run and observed climate from random fluctuations; this is particularly true for the higher order autocorrelation coefficients. Especially for short simulation runs large differences can be found between standard deviations and the autocorrelation coefficients for successive months. It is advisable to make comparisons on a seasonal basis instead of on monthly bases in such cases.

4. Sea surface temperature

4.1 Average sea surface temperature

Sea surface temperatures are overestimated by about 1-3 ℃ in the GCM control run, see Table 5. Wilson and Mitchell [1] found sea surface temperatures outside the tropics to be generally larger than observed. It is remarkable that for the GCM control experiment almost all average sea surface temperatures are systematically 0.1 ℃ higher than the average surface air temperatures given in Table 1.

TABLE 5. *Average sea surface temperature* (℃)

GRID	Land Sea	DEC		JAN		FEB	
		GCM	Obs.	GCM	Obs.	GCM	Obs.
4807[1)]	s	10.8	8	9.5	6	8.8	6
0107[2)]	s	9.1	–	7.9	–	6.8	6.3
4809[7)]	s	13.7	11	12.6	10	12.4	10

Obs. [1)]*Aberdeen (GB) 1931-60* [5]; [2)]*North Sea, 1961-80* [6];
[7)]*Belle-Île (F) 1931-60* [5].

4.2 Standard deviation of monthly means

The standard deviations of monthly sea surface temperatures are presented in Table 6. Note that for the model simulation the standard deviations of the sea surface temperature almost exactly match those of the surface air temperature (Table 2).

TABLE 6. *Standard deviation of monthly sea surface temperatures* (℃)

GRID	Land Sea	DEC		JAN		FEB	
		GCM	Obs.	GCM	Obs.	GCM	Obs.
4807	s	0.8	–	0.9	–	0.9	–
0107[2)]	s	1.2	–	0.9	–	1.0	0.7
4809	s	1.1	–	1.5	–	1.2	–

Obs. [2)]*North Sea, 1961-80* [6];

5. Precipitation

The GCM results in this chapter have been multiplied with a factor to give the correct number of days in each month i.e. 31 days for December and January and 28.25 days for February.

5.1 Average monthly precipitation

The average monthly precipitation amount (large scale rain, convective rain and snowfall) is shown in Table 7. For 15 out of 24 comparable month/grid point combinations the average precipitation amount in the GCM control experiment is smaller than observed. Some of the extreme differences, for example for grid points 4808 and 0209, may be attributed to orographic effects.

TABLE 7. *Average monthly precipitation amount (mm)*

GRID	Land Sea	DEC		JAN		FEB	
		GCM	Obs.	GCM	Obs.	GCM	Obs.
4807[1]	S	66	80	58	78	45	55
0107	S	75	-	64	-	46	-
0207[3]	L	41	41	33	48	28	31
4808[4]	L	33	96	35	97	26	72
0108[5]	L	31	79	53	67	34	50
0208[6]	L	43	41	48	37	38	33
4809[7]	S	88	82	88	72	86	52
0109[8]	L	50	70	68	67	71	55
0209[9]	L	69	80	66	105	63	92

Obs. [1]*Aberdeen (GB) 1931-60* [5]; [3]*Skagen (DK), 15 years* [7];
[4]*Aberystwyth (GB), 1931-60* [7]; [5]*De Bilt (NL), 1951-80* [9];
[6]*Lüchow (D), 1931-60* [7]; [7]*Belle-Île (F) 1931-60* [5];
[8]*Nevers (F), 1931-60* [7]; [9]*Bad Tölz (D), 1931-60* [7].

5.2 Average number of days with precipitation

A precipitation day is defined as a day with measurable rainfall. The lowest precipitation amount measured by a rain gauge at an observational station is usually 0.05 mm for the continent and 0.005 inch (= 0.12 mm) for GB, which are recorded (rounded) as 0.1 mm and 0.01 inch respectively. For comparison the threshold for the GCM simulation is chosen to be also 0.05 mm for the continental grid points and 0.005 inch for the two British grid points. The results are given in Table 8, which shows very marked differences between the observed and the simulated number of days with precipitation. The average number of precipitation days in the GCM control run exceeds the observed average number in 23 out of 24 cases. Quite often the number of

days with precipitation in the GCM run is about twice as large as the observed number.

TABLE 8. *Average number of days per month with precipitation ≥ 0.05 mm (with asterisk ≥ 0.005 inch)*

GRID	Land Sea	DEC		JAN		FEB	
		GCM	Obs.	GCM	Obs.	GCM	Obs.
4807[1]	S	30*	18*	29*	19*	27*	16*
0107	S	31	-	31	-	28	-
0207[3]	L	27	12	24	12	20	9
4808[4]	L	21*	22*	24*	21*	24*	17*
0108[5]	L	26	21	30	21	24	19
0208[6]	L	30	14	30	15	26	13
4809[7]	S	31	16	31	17	28	12
0109[8]	L	26	16	29	17	27	15
0209[9]	L	28	15	30	16	27	15

Obs. [1] *Aberdeen (GB) 1931-60* [5]; [3] *Skagen (DK), 15 years* [7];
[4] *Aberystwyth (GB), 1931-60* [7]; [5] *De Bilt (NL), 1931-60* [8,Vol.5];
[6] *Lüchow (D), 1931-60* [7]; [7] *Belle-Île (F) 1931-60* [5];
[8] *Nevers (F), 1931-60* [7]; [9] *Bad Tölz (D), 1931-60* [7].

So averaged over the whole grid there are too many days with little precipitation in the GCM control simulation compared with the observations. This is in agreement with the findings of Wilson and Mitchell [2] who used a 5-layer version of the UKMO GCM.

The overestimation of the number of wet days can partly be a result of the areal averaging. Usually the GCM value at a grid point is considered to represent the areal average over the entire grid box area. The number of days with precipitation in an area is generally larger than that observed at a single point. An example of the effect of spatial averaging on the frequency of wet days can be found in Reed [14]. He showed that for England and Wales the average number of wet days over large areas still remained below that produced by a 5-layer version of the UKMO GCM. In contrast to Reed [14] Table 8 only refers to the winter period. In the Netherlands the spatial correlation of precipitation in winter is stronger than in other seasons [15]. The frequency of days with average precipitation ≥ 0.05 mm over the Netherlands is in winter about 30 % higher than that at a single point [16]. The size of the GCM grid boxes, however, is about 8 times the size of the Netherlands This indicates that a considerable part of the differences in Table 8 can be attributed to spatial averaging. It is however unlikely that the average difference of about 70 % can be attributed to spatial averaging alone.

Besides too few days without precipitation the GCM simulates almost no days with heavy precipitation (≥ 10.0 mm) while the observations show a monthly average of one or two of these days. Reed [14] found too few days with precipitation above 20.0 mm for Eastern England.

It rains almost every day at the sea points in the GCM control run in Table 8. The large mean monthly precipitation amount at the sea points compared with the land points is not only caused by the larger number of days with precipitation, but also by a larger precipitation intensity.

5.3 Large scale rain, convective rain and snowfall

The mean winter precipitation amount for the three different types of precipitation in the GCM averaged over land and sea points respectively is given in Table 9. The differences in convective precipitation and snowfall between land points and sea points are noticeable. At sea points there is about five times more convective precipitation than at land points. This is consistent with Figure 3, which indicates deep convection over sea even in the mean situation. For land points snowfall contributes more than half of the total precipitation whereas for sea points there is almost no snowfall at all. This is in agreement with the large temperature differences between land and sea points.

TABLE 9. *GCM average winter (DJF) precipitation (mm)*

	land points Av.	sea points Av.
Large scale rain	30.3	42.3
Convective rain	27.3	161.1
Snowfall	80.1	1.2
Total precipitation	137.7	204.6

6. Global radiation

The global radiation is the incoming solar radiation at the surface. To make a fair comparison between monthly sums the GCM results are transformed to the correct number of days in each month as before.

6.1 Average monthly global radiation

The observed and simulated average global radiation are presented in Table 10. In 12 out of 19 comparable cases the monthly average of the GCM run is larger than the observed average. However, even at the 20%-level this result is not significant. Due to the increasing solar declination the observations show from January to February about a doubling of the global radiation. This feature is correctly simulated by the GCM control run.

TABLE 10. *Average monthly global radiation (MJ/m^2)*

GRID	Land Sea	DEC		JAN		FEB	
		GCM	Obs.	GCM	Obs.	GCM	Obs.
4807[1]	S	44.9	±27	59.6	-	128.0	-
0107	S	35.0	-	51.7	-	115.3	-
0207[3]	L	32.5	30.2	56.0	47.1	113.7	114.0
4808[4]	L	91.3	62.6	92.4	78.8	165.6	151.2
0108[5]	L	70.2	56.4	48.7	70.1	128.6	129.7
0208[6]	L	51.0	38.6	63.7	52.0	114.4	111.0
4809	S	104.4	-	119.5	-	173.5	-
0109[8]	L	109.4	80.0	93.0	108.9	145.8	190.2
0209[9]	L	80.4	70.4	72.5	89.3	133.0	168.4

Obs. [1]*Aberdeen (GB) >10 years* [17];
[3]*Mean of Copenhagen (DK) and Oslo (N) 1931-60* [8,Vol.5];
[4]*Aberporth (GB), 1959-68* [8,Vol.5]; [5]*De Bilt (NL), 1961-80* [18];
[6]*Mean of Hamburg (D), Berlin (D) and Braunlage (D) 10 years* [7];
[8]*Mean of Paris (F), Limoges (F) and Lyon (F)* [7];
[9]*Weihenstephan (D) 10 years* [7].

6.2 Standard deviation of monthly sums

The standard deviations of monthly global radiation for De Bilt (NL) [18] and those of the GCM control run are given in Table 11. For February the difference is just significant at the 10%-level. Application of the test to the sum of the variances for the three months yields a value which is only close to significance at the 10%-level.

TABLE 11. *Standard deviation of monthly global radiation (MJ/m^2)*

GRID	Land Sea	DEC GCM	DEC Obs.	JAN GCM	JAN Obs.	FEB GCM	FEB Obs.
0108[5]	L	9.8	8.8	9.5	13.9	34.4‡	20.0

Obs. [5]*De Bilt (NL), 1961-80* [18].
‡*Standard deviations significantly different at the 10 % - level according to the F-test.*

7. 500 mbar circulation

Charts of the mean 500 mbar geopotential height and the resultant wind direction at 500 mbar for January, February and December, averaged over the 5 simulated years are shown in Figure 4. The wind direction at 500 mbar is calculated here as the average of the wind at layer 7 and 6 with σ is 0.577 and 0.436 respectively. As before, these plots are calculated with 25 instead of 9 GCM grid points. The GCM simulation is compared with the results of an average of 8 years ECMWF analyses of the 500 mbar geopotential height for the three months projected onto the model grid, presented in Figure 5.

The simulated 500 mbar height shows a spurious trough over the North Sea for all three months. It is very likely that this trough is caused by the rising air over the warm sea surface (see also Figure 3 section 3.2). The north-component of the 500 mbar height of the GCM control experiment is strong compared with the ECMWF analysis. This is true particularly for December. The total gradient over the study area and hence the wind speed at the 500 mbar height is realistically simulated.

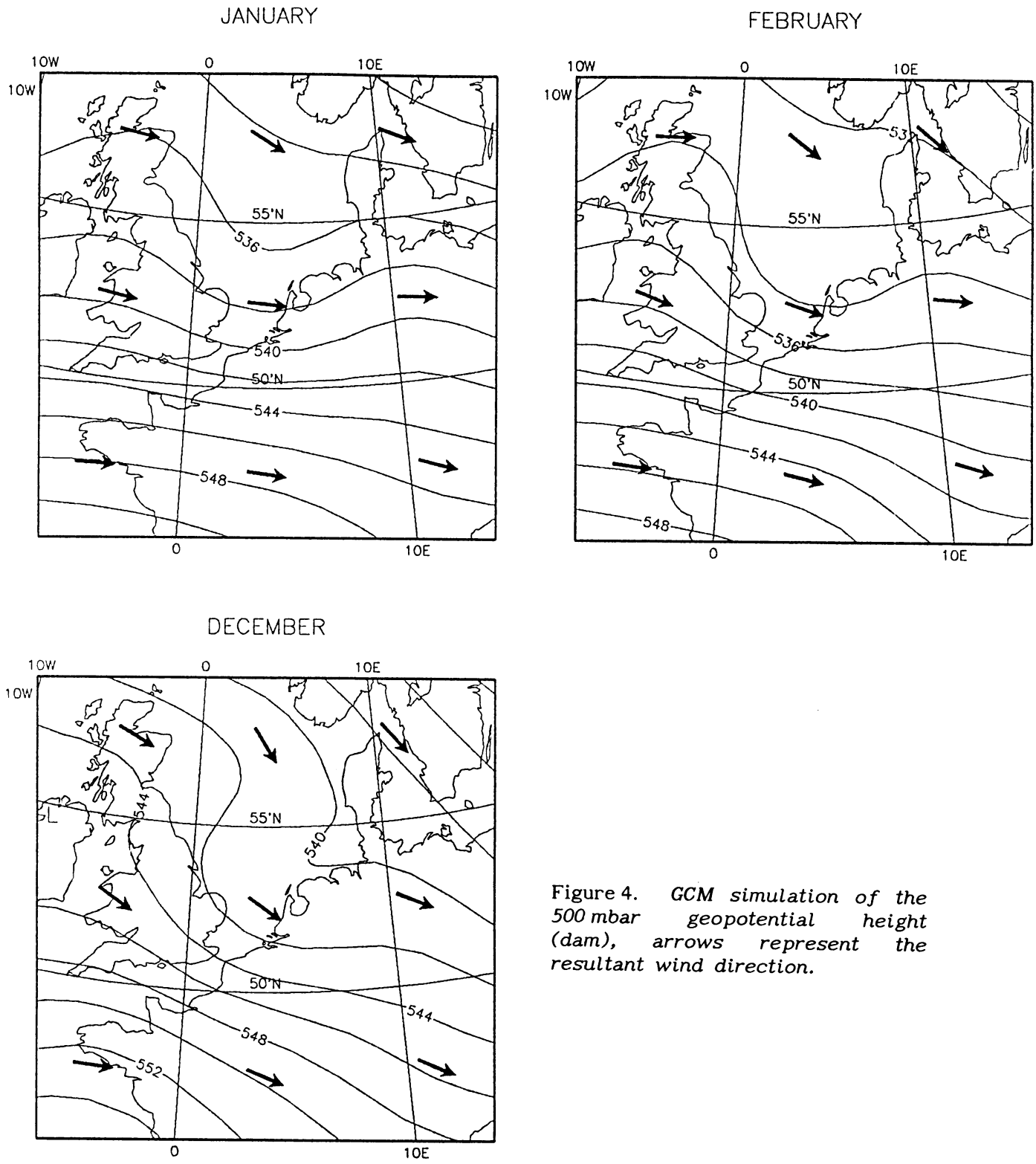

Figure 4. *GCM simulation of the 500 mbar geopotential height (dam), arrows represent the resultant wind direction.*

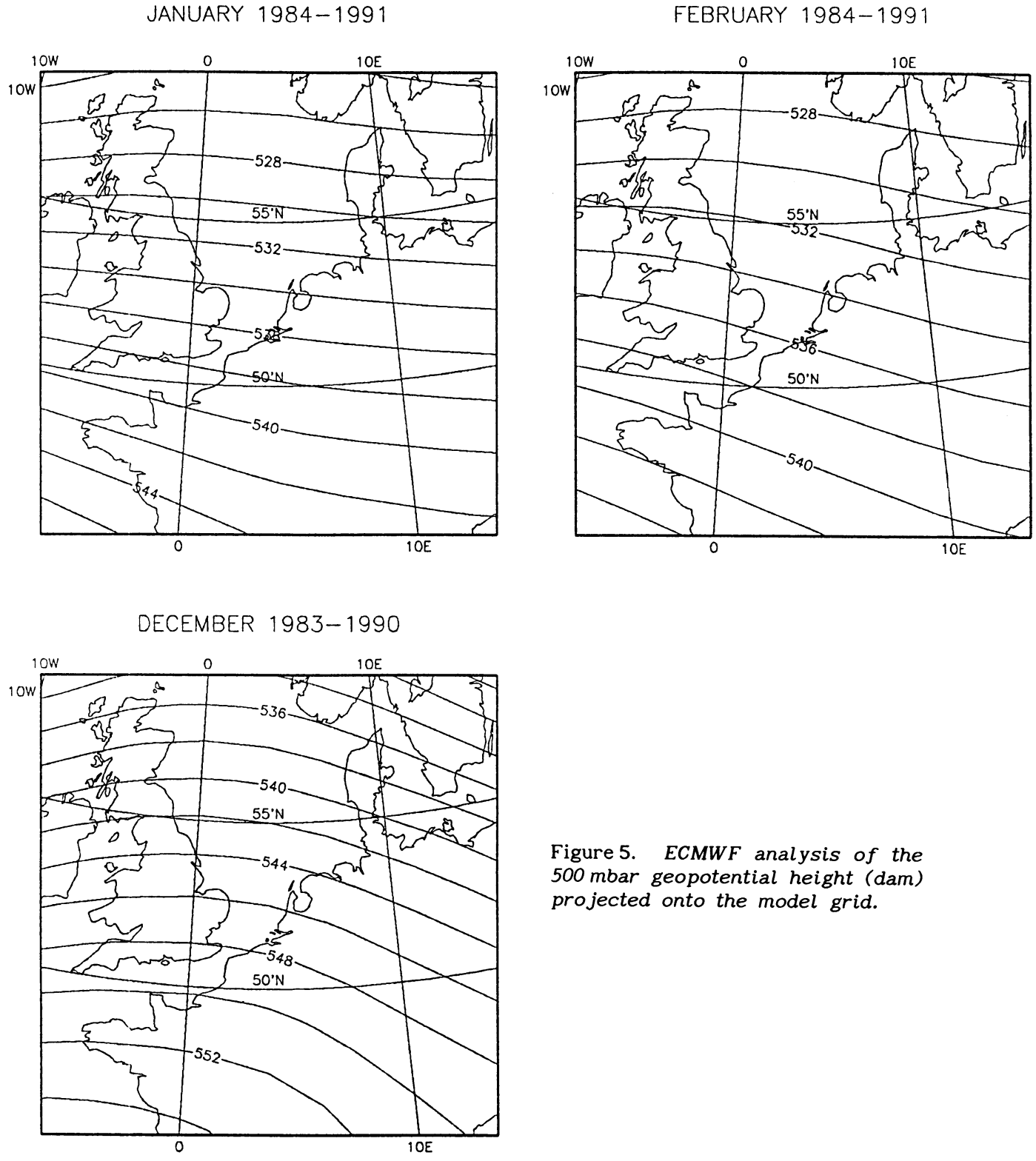

Figure 5. *ECMWF analysis of the 500 mbar geopotential height (dam) projected onto the model grid.*

8. Sea level pressure

8.1 Mean sea level pressure

The pressure given by the model is the midnight surface pressure. This surface pressure is reduced daily to the sea level pressure according to WMO standards [19]. Here, the temperature correction is taken into account but not the effect of humidity which is important in (sub)tropical regions only.

Table 12 gives the mean sea level pressure for both GCM control run and observations. In December the sea level pressures of the GCM simulation are slightly higher than the observed ones, in January and February the reverse is true. For 6 out of 24 cases the mean sea level pressure of the GCM run is larger than observed. For independent data this result is just significant at the 5%-level but it will be no longer significant if the effect of strong spatial correlation of the sea level pressure is taken into account.

TABLE 12. *Mean sea level pressure (mbar)*

GRID	Land Sea	DEC		JAN		FEB	
		GCM	Obs.	GCM	Obs.	GCM	Obs.
4807[1]	S	1012.9	1008.2	1006.8	1009.4	1004.1	1011.4
0107	S	1014.9	-	1009.0	-	1007.8	-
0207[3]	L	1017.5	1010.1	1012.5	1012.6	1012.0	1015.2
4808[4]	L	1015.4	1013.7	1008.6	1011.6	1005.4	1012.2
0108[5]	L	1017.7	1013.6	1010.1	1014.2	1007.7	1014.1
0208[6]	L	1019.6	1015.7	1014.1	1015.8	1011.5	1015.1
4809[7]	S	1011.7	1018.0	1009.1	1015.4	1006.8	1014.3
0109[8]	L	1018.9	1020.6	1013.7	1018.8	1010.2	1016.7
0209[9]	L	1020.3	1019.3	1015.6	1019.4	1010.8	1018.6

Obs. [1]*Aberdeen (GB), 1931-60* [20]; [3]*Göteborg (S), 1971-80* [20];
[4]*Average of Birmingham (GB) and Rosslare (IRL), 1971-80* [20];
[5]*De Bilt (NL), 1951-80* [9]; [6]*Potsdam (D), 1931-60* [20];
[7]*Average of Nantes (F) and Brest (F), 1971-80* [20];
[8]*Dijon (F), 1971-80* [20]; [9]*Munich (D), 1931-60* [20].

To get an impression of the geographical pressure distribution, plots of the mean sea level pressure including the resultant wind direction in the bottom model layer ($\sigma = 0.987$) were made for the GCM simulation. Figure 6 displays the circulation patterns of January, February and December respectively. Again these patterns are calculated with 25 instead of 9 grid points. ECMWF analyses of the mean sea level pressure averaged over 8 years for each month and projected onto the model grid are presented in Figure 7. The simulated patterns have a stronger south-component and show some strong waves compared with the rather smooth ECMWF analysis. These waves seem to be related with the temperature gradient between land and sea. During December

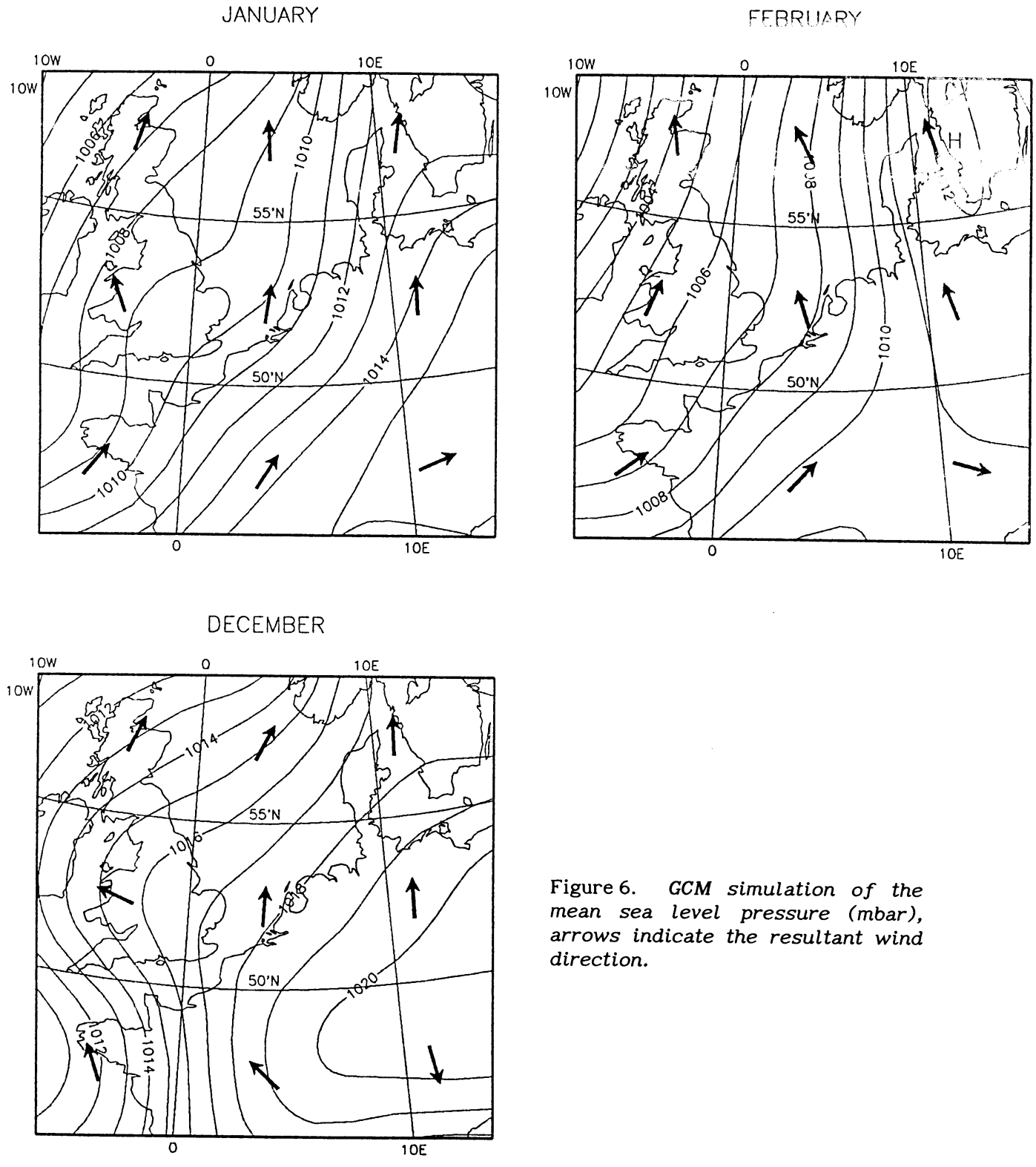

Figure 6. *GCM simulation of the mean sea level pressure (mbar), arrows indicate the resultant wind direction.*

and January the simulated pressure gradient is about 50% smaller than observed. The observed high pressure region in the south-east of the study area is for none of the three months simulated properly.

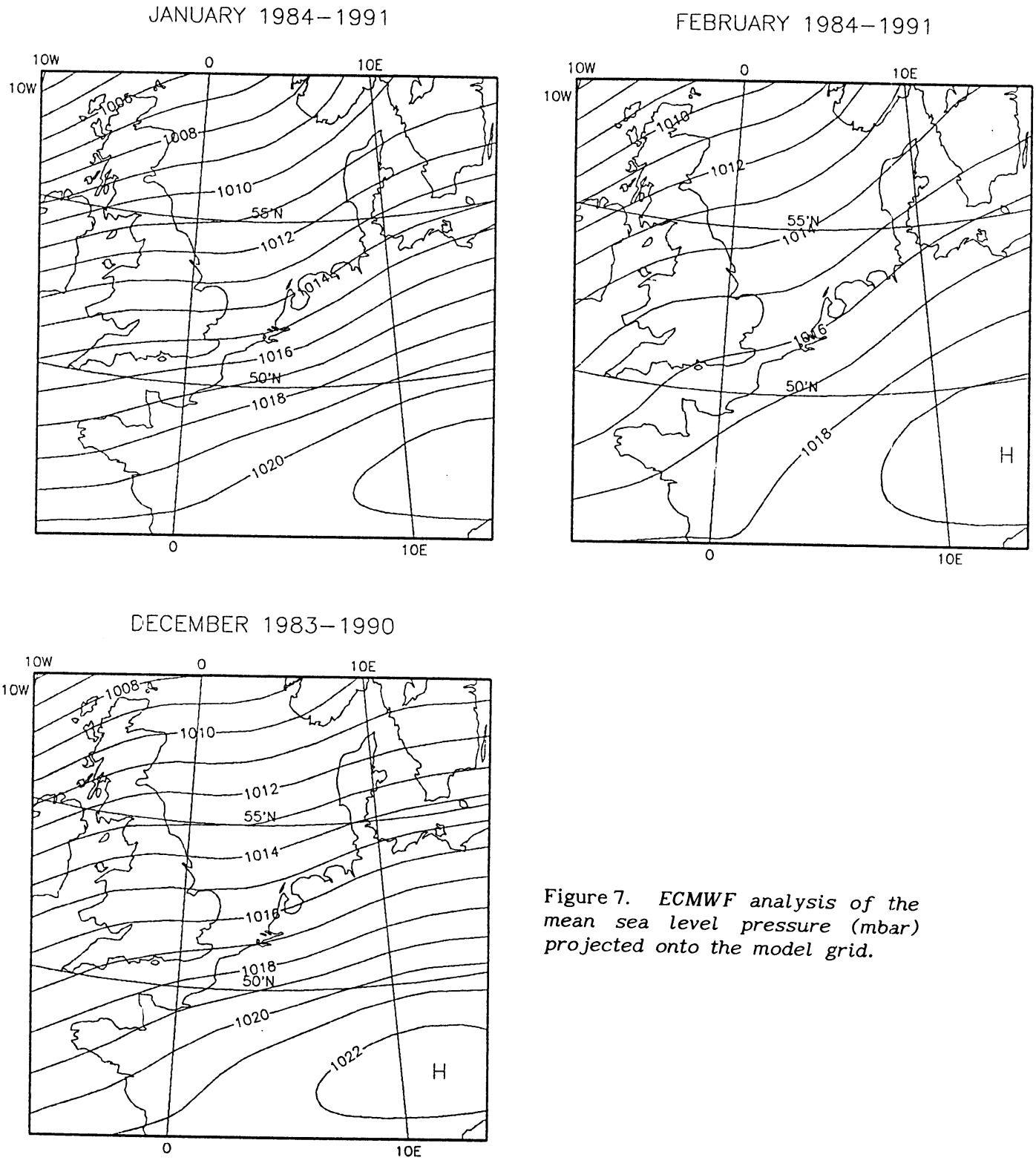

Figure 7. *ECMWF analysis of the mean sea level pressure (mbar) projected onto the model grid.*

8.2 Standard deviation of monthly and daily means

The standard deviations of the monthly pressure of the GCM control run and the observations for De Bilt are shown in Table 13. The standard deviations for the GCM simulation are smaller than those for the observed sea level pressure. For individual months the value of the F-statistic is not significant at the 10%-level, but application of the test to the sum of the variances for the three months results in a value which is just significant at the 5%-level.

TABLE 13. *Standard deviation of monthly sea level pressure (mbar)*

GRID	Land Sea	DEC		JAN		FEB	
		GCM	Obs.	GCM	Obs.	GCM	Obs.
0108[5]	L	3.1	6.0	4.2	5.1	3.3	6.9

Obs. [5]*De Bilt (NL), 1951-80* [9].

Standard deviations of daily sea level pressure, which represent the daily variability, for De Bilt (NL) and the GCM simulation are given in Table 14. As for the standard deviations of the monthly sea level pressure the daily pressure variability is underestimated in the GCM control experiment. This is however just the opposite of the daily surface temperature variability which, as we remember, is overestimated in the GCM simulation (Table 3).

TABLE 14. *Standard deviation of daily sea level pressure (mbar)*

GRID	Land Sea	DEC		JAN		FEB	
		GCM	Obs.	GCM	Obs.	GCM	Obs.
0108[5]	L	9.9†	13.0	10.1†	12.4	8.9†	13.2

Obs. [5]*De Bilt (NL), 1951-80*
†*Standard deviations significantly different at the 1% - level.*

Differences in the daily variability of the sea level pressure are again tested with a modification of the Katz [11] procedure as outlined in the Appendix. When a second order autoregressive model is fitted to both GCM simulation and observations the standard deviations of the daily sea level pressure are significantly different at the 1% - level for all three months.

8.3 Autocorrelation

The autocorrelation coefficients of the GCM control run decrease more rapidly with increasing lag than those of the observational data from De Bilt especially during December and January, which is shown in Table 15. According to Bartlett's formula the standard errors of the first-order autocorrelation coefficients of the simulation are about 0.03 and those of the observations about 0.02. The standard errors in Table 15 are calculated with the jackknife. The first-order autocorrelation coefficients do not differ significantly. As expected the observations show a weaker autocorrelation for the sea level pressure compared with the surface temperature (Table 4). This feature is also present in the GCM simulation.

TABLE 15. *Autocorrelation coefficients of daily sea level pressure*

	DEC		JAN		FEB	
LAG	GCM	Obs.	GCM	Obs.	GCM	Obs.
1	0.80±0.03	0.79±0.02	0.76±0.09	0.78±0.02	0.82±0.01	0.83±0.02
2	0.43±0.09	0.54±0.04	0.40±0.21	0.52±0.04	0.56±0.02	0.61±0.03
3	0.09±0.13	0.38±0.05	0.18±0.24	0.33±0.06	0.32±0.04	0.45±0.05
4	-0.12±0.15	0.25±0.05	0.09±0.20	0.21±0.07	0.13±0.07	0.34±0.05
5	-0.20±0.13	0.16±0.05	0.05±0.16	0.14±0.07	-0.02±0.09	0.27±0.06
6	-0.18±0.08	0.09±0.06	0.04±0.12	0.11±0.06	-0.12±0.10	0.20±0.06
7	-0.08±0.06	0.03±0.06	0.04±0.07	0.08±0.06	-0.17±0.12	0.14±0.06
8	0.04±0.11	-0.02±0.06	-0.01±0.06	0.07±0.06	-0.17±0.13	0.11±0.06
9	0.10±0.12	-0.04±0.05	-0.05±0.08	0.06±0.05	-0.17±0.14	0.09±0.06
10	0.06±0.09	-0.04±0.05	-0.06±0.08	0.04±0.05	-0.15±0.14	0.06±0.06

GCM *GCM control run results from grid point 0108*
Obs. *Observations from De Bilt (NL) period 1951-80*
The standard errors of the autocorrelation coefficients are calculated with the Jackknife [12].

9. Wind

9.1 Average 100 m wind speed and average geostrophic wind speed

The bottom model layer at which the wind is calculated has a σ level equal to 0.987. For a surface pressure of 1000 mbar this corresponds to a height of about 100 m above sea level. In the model the roughness length z_0 is 0.1 m over land and 0.0001 m over sea. For most grid points, observed 100 m winds are not available. Table 16 shows for two grid points the 100 m midnight GCM winds and the observations at platform K13 (76 m) and Cabauw (80 m, z_0 = 0.15 m).

TABLE 16. *Average 100 m wind speed (m/s) and average wind direction*

GRID	Land Sea	DEC		JAN		FEB	
		GCM	Obs.	GCM	Obs.	GCM	Obs.
0107[2)]	S	8.7	11.9	7.9	12.1	8.2	11.2
		212	248	185	241	152	204
0108[5)]	L	5.6	8.6	5.7	8.8	6.0	9.1
		179	228	182	216	165	209

Obs. [2)]*platform K13, 76m above ground level (2400GMT), 1982-1990;*
[5)]*Cabauw (NL), 80m above ground level (2400GMT), 5 years.*

Table 16 indicates a backed GCM wind which is consistent with the flow patterns of Figures 6 and 7. The GCM underestimates the wind speed by about 30 %. A part of this difference can be explained from an underestimation of the geostrophic forcing. Table 17 compares the average geostrophic wind speeds of the GCM, calculated from the daily pressure fields, with those calculated from 8 years ECMWF analysis.

TABLE 17. *Average geostrophic wind speed (m/s)*

GRID	Land Sea	DEC		JAN		FEB	
		GCM	ECMWF	GCM	ECMWF	GCM	ECMWF
4807	S	9.5	11.5	8.4	12.3	10.3	11.7
0107	S	10.7	10.9	9.5	11.4	9.9	10.5
0207	L	10.0	9.9	9.5	10.4	9.1	9.4
4808	L	8.9	10.7	9.1	11.5	8.6	11.6
0108	L	8.9	10.8	9.8	11.3	9.4	10.9
0208	L	10.3	10.6	11.1	11.1	9.4	10.2
4809	S	11.1	10.1	10.5	10.7	8.4	10.0
0109	L	10.4	8.1	9.4	9.2	8.3	8.9
0209	L	9.8	7.8	8.6	8.0	8.7	8.0

ECMWF: *8 years analysis (1983-1991).*

The average GCM geostrophic forcing is 5 % smaller over land and 11 %

smaller over sea than the ECMWF values; for grid points 0108 and 0107 the underestimation is 15 % and 8 % respectively. Hence this underestimation of the geostrophic wind explains only part of the differences in Table 16. Table 18 shows the average winter (DJF) wind speeds of Table 16. The GCM wind speeds are scaled up with the ratio of observed and simulated geostrophic forcing from Table 17. The Cabauw observations are transformed to 100 m and $z_0 = 0.1$ m assuming neutral stability [22]. For platform K13 no transformation is applied, because the boundary layer over sea is unstable in winter and a transformation from 76 to 100 m would have little effect. After these corrections, it turns out that the underestimation of the wind speed is for both grid points of the same order. Apparently, the extremely high stability over land (Figure 3) does not affect the created 100 m wind speed significantly.

TABLE 18 *Corrected average DJF 100 m wind speeds (m/s)*

GRID	Land Sea	GCM	Observation	Difference (%)
0107[2)]	S	9.0	11.7	23
0108[5)]	L	6.8	9.7	30

Obs. [2)]*platform K13, (2400GMT), 1982-1990*
[5)]*Cabauw (NL), (2400GMT), 5 years.*

9.2 Wind distribution

Tables 19 and 20 compare the wind distribution of the 100 m GCM wind at grid point 0108 with the 10 m Schiphol (NL) observations. Since the backing due to friction occurs mainly above 100 m [23], it is justified to compare the data of the two heights in Table 19. The frequency distribution of the wind directions shows that the difference in mean wind direction (Table 16) is partly a result of the relatively high frequencies for south-eastern wind directions in the GCM. For all three months the sectors in which the highest observed mean wind speeds are found are west and west-south-west. For the GCM the sector with the maximum wind speed is south for December and January and north-north-east for February though it should be said that for February the frequency of this sector is only 1.3 %.

TABLE 19. *Frequencies of wind directions (%)*

DIR	DEC		JAN		FEB	
	GCM	Obs.	GCM	Obs.	GCM	Obs.
0	8.7	3	4.7	3	1.3	5
30	7.3	2	5.3	3	1.3	6
60	4.0	6	7.3	7	5.3	**12**
90	6.7	8	9.3	8	14.7	10
120	10.7	6	12.0	6	**19.3**	6
150	12.7	9	7.3	10	6.7	8
180	8.7	13	9.3	14	9.3	10
210	**14.0**	**18**	**18.0**	**15**	14.0	11
240	7.3	13	12.7	12	11.3	11
270	10.7	9	8.0	9	10.0	8
300	4.0	6	4.0	6	3.3	5
330	4.0	4	1.3	5	2.7	6
VAR	1.3	3	0.7	3	0.7	3

GCM *GCM control run results from grid point 0108*
Obs. *Observations from Schiphol (NL) period 1951-1980* [9]
VAR *GCM: wind velocities ≤ 1.0 m/s; Obs.: calm or direction not determinable*

TABLE 20. *Mean wind speed per direction (m/s)*

DIR	DEC		JAN		FEB	
	GCM	Obs.	GCM	Obs.	GCM	Obs.
0	5.4	4	5.1	4.5	5.0	4.5
30	5.4	4.5	5.8	5	8.7	5.5
60	4.2	6	4.3	6	5.1	6
90	4.7	4.5	5.2	5.5	6.0	5
120	5.6	4.5	5.6	4.5	6.5	4
150	5.6	5	5.2	5.5	5.6	5
180	6.3	5.5	6.6	5.5	6.1	5.5
210	6.3	6.5	6.3	6.5	5.2	6
240	5.4	7.5	5.5	7.5	6.4	7
270	5.2	7.5	6.3	7.5	5.9	7
300	5.6	7	5.1	7	5.2	6
330	5.7	5.5	6.3	5.5	7.4	5.5

GCM *GCM control run results from grid point 0108*
Obs. *Observations from Schiphol (NL) period 1951-1980* [9]

10. Discussion and conclusions

On several aspects, there are large differences between the control run in the NW European region and the observed climate. For temperature there is a large underestimation by the GCM over land. Over sea however, the model overestimates the temperature. Although the GCM pressure maps indicate a South to South-Western airflow, there is no indication that the sea points are affected by the advection of cold (model-) air from land. Rather, it seems that an instantaneous equilibrium is created by the boundary layer physics as soon as the air reaches sea and vice versa.

The high air temperature near the sea surface leads to an enhanced vertical instability. As a result of this effect more showers should be generated over sea. Indeed this is consistent with the precipitation data which show both more days with (convective) precipitation and higher precipitation intensities at sea points.

It seems likely that the creation of the 500 mbar trough and the remarkable behaviour of the surface temperature from sea to land are both related with the way surface physics is represented in the model; the sea surface temperature and the air temperature over the sea surface are very closely connected. Apparently, the difference in surface physics over land and sea creates a kind of heat low in the air flow.

The mean sea level circulation patterns have a too strong south-component whereas the 500 mbar flow patterns show a too strong north-component compared with observations. This means that the wind veers too much with increasing altitude.

The standard deviation of the GCM monthly sea level pressure is underestimated by a factor two. The standard deviation of the daily sea level pressure is significantly underestimated. This underestimation is possibly due to the coarse mesh of the model. According to the IPCC-report [24] however, the daily variability of the sea level pressure is in most GCMs well simulated. The simulated first-order autocorrelation coefficients are realistic. Apparently, effects of short time scale like eddy propagation are described properly. The small higher order autocorrelation coefficients (lag 3 and beyond) on the other hand indicate that processes of larger time scale, such as the life cycle of large meteorological systems, are not correctly reproduced by the model.

In contrast with the sea level pressure the standard deviation of the daily surface temperature is overestimated which is commonly found for GCMs [24], [10]. Grid point 0108 shows compared with De Bilt for December and

February a realistic value of the standard deviation of the monthly surface temperature. However, from Table 4 it is clear that this happens only by virtue of the above mentioned underestimation of the autocorrelation coefficients beyond time lags of 3 days.

GCM simulations exhibit random fluctuations from year to year in a similar way to the observed climate. Over a period of only five years these fluctuations are not unimportant, the "realistic" January autocorrelation coefficients of the surface temperature may therefore have arisen by chance. For relatively short simulation runs it is preferable to make comparisons on a seasonal basis.

In summary. Apart from systematic errors the GCM control simulation also contains random fluctuations resulting from the short simulation run. Obviously, care should be taken in using time series generated by a GCM on a local scale. The aim of the present study was to develop tools for analyzing GCM time series. Future work will cover i) the other seasons, ii) the difference between the $2xCO_2$ and $1xCO_2$ runs and iii) (other) models preferably with a simulation period of at least 10 years and higher resolution.

Acknowledgement

The Hadley Centre for Climate Prediction and Research is acknowledged for providing the data of a version of the UKMO 11-layer model. I would like to thank T.A. Buishand and G.P. Können for many fruitful discussions and suggestions, the KNMI Climatological Service for providing observed data of De Bilt and platform K13 and the KNMI Studio for drawing Figure 3.

Appendix

Real and simulated atmospheric time series are autocorrelated, therefore the variance of an underlying uncorrelated process, called the innovation variance is considered instead of the variance of the original process. The method is analogous to that described by Katz [11] but slightly modified to avoid the use of zero starting values.

It is assumed that the climate time series can be represented by an autoregressive process of order p, $p \geq 1$, denoted by AR(p). Let $x_{i,j}$ denote a climate variable on day i ($i=1,\ldots,n$) of a certain month in year j ($j=1,\ldots,m$). For an AR(p) process the time series $x_{i,j}$ with mean μ and variance σ^2 can be expressed as

$$x_{i,j} - \mu = \sum_{k=1}^{p} \phi_k (x_{i-k,j} - \mu) + a_{i,j} \; . \tag{1}$$

Here ϕ_k, $k=1,\ldots,p$ are the autoregression coefficients. The $a_{i,j}$'s are called innovations and constitute an uncorrelated process with zero mean and constant variance σ_a^2.

The order p of the autoregressive process can be determined with the Bayesian Information Criterion [25]. If the order p of the AR(p) process is known, estimates of the autoregression coefficients $\hat{\phi}_k$, $k=1,\ldots,p$ can be obtained from the first p estimated autocorrelation coefficients. Substituting the estimates $\hat{\phi}_k$ for ϕ_k and the time average $\bar{x}$ for μ the estimated innovations are given by

$$\hat{a}_{i,j} = (x_{i,j} - \bar{x}) - \sum_{k=1}^{p} \hat{\phi}_k (x_{i-k,j} - \bar{x}), \quad i=p+1,\ldots,n; \; j=1,\ldots,m. \tag{2}$$

The use of $x_{i-k,j} = \bar{x}$ if $i-k \leq 0$, as is sometimes proposed in the literature, can lead to anomalous values of $\hat{a}_{1,j},\ldots,\hat{a}_{p,j}$. In contrast with Katz [11] the $\hat{a}_{i,j}$'s for $i \leq p$ are therefore not considered. An estimator $\hat{\sigma}_a^2$ of the innovation variance is

$$\hat{\sigma}_a^2 = \frac{1}{(n-p)m} \sum_{i=p+1}^{n} \sum_{j=1}^{m} \hat{a}_{i,j}^2. \tag{3}$$

When two mutually independent time series are compared the problem of concern is to make inferences about the unknown difference between the innovation variances, $\sigma_a^2(1)$ and $\sigma_a^2(2)$. Under the null hypothesis ($\sigma_a^2(1) = \sigma_a^2(2)$), the distribution of the statistic

$$Z = \frac{\ln \hat{\sigma}_a^2(1) - \ln \hat{\sigma}_a^2(2)}{\{s^2[\ln \hat{\sigma}_a^2(1)] + s^2[\ln \hat{\sigma}_a^2(2)]\}^{1/2}} \tag{4}$$

is approximately standard Gaussian for large sample sizes. Here the variance of $\ln\hat{\sigma}_a^2$ is according to Davis [26] estimated by:

$$s^2[\ln\hat{\sigma}_a^2] = \frac{2 + \hat{\gamma}_2}{(n-p)m}. \tag{5}$$

In Eq. (5) $\hat{\gamma}_2$ is the sample kurtosis which is a measure of the peakedness or flatness of a distribution relative to the Gaussian. The sample kurtosis is given by

$$\hat{\gamma}_2 = \frac{\frac{1}{(n-p)m}\sum_{i=p+1}^{n}\sum_{j=1}^{m}\hat{a}_{i,j}^4}{\left(\frac{1}{(n-p)m}\sum_{i=p+1}^{n}\sum_{j=1}^{m}\hat{a}_{i,j}^2\right)^2} - 3 \tag{6}$$

with the innovations $\hat{a}_{i,j}$ specified by Eq. (2).

Table A1 gives the variances (of the original process), the innovation variances and the Z-statistics of GCM grid point 0108 and De Bilt observations for the surface air temperature and the sea level pressure. All time series were represented by AR(2) processes. The critical values of $|Z|$ are 2.576, 1.960 and 1.645 for tests at the 1 %, 5 % and 10 % significance level respectively.

TABLE A1. *Variances, Innovation variances and Z-statistics*

		DEC		JAN		FEB	
		GCM	Obs.	GCM	Obs.	GCM	Obs.
σ^2	T	39.23	16.74	47.00	17.24	41.35	17.08
$\hat{\sigma}_a^2$	T	8.99	5.40	5.77	4.99	4.97	3.88
Z	T	3.36		0.79		1.72	
σ^2	P	98.35	169.43	101.33	152.09	77.97	176.15
$\hat{\sigma}_a^2$	P	15.53	49.76	23.36	49.34	12.52	43.26
Z	P	-9.15		-3.26		-9.83	

GCM *GCM control run results for grid point 0108*
Obs. *Observations from De Bilt (NL) period 1951-1980*
T *Surface air temperature*
P *Sea level pressure*

For the surface air temperature the difference in (innovation) variance is significant at the 1 % - level for December and at the 10 % - level for February. The differences in sea level pressure variability are significant at the 1 % - level for all three months.

References

[1] Wilson, C.A. and Mitchell, J.F.B.
A doubled CO_2 climate sensitivity experiment with a GCM including a simple ocean
Journal of Geophysical Research, 92, D11, 13,315-13,343, 1987.

[2] Wilson, C.A. and Mitchell, J.F.B.
Simulated climate and CO_2-induced climate change over Western Europe
Climate Change, 10, 11-42, 1987.

[3] Slingo, A (Ed.)
Handbook of the Meteorological Office 11-layer atmospheric general circulation model, Met. O. 20 DCTN 29
Meteorological Office, Bracknell, England (unpublished), 1985.

[4] Parton, W.J. and Logan, J.A.
A model for diurnal variation in soil and air temperature
Agricultural Meteorology, 23, 205-216, 1981.

[5] Deutscher Wetterdienst
Klimadaten von Europa, Teil I: Nord-, West- und Mitteleuropa
Bearbeitet von M. Kalb und H. Noll
Deutscher Wetterdienst, Offenbach am Main, 1990.

[6] Korevaar, C.G.
North Sea Climate based on observations from ships and lightvessels
Kluwer academic publishers, Dordrecht, 1990.

[7] Müller, M.J.
Handbuch ausgewählter Klimastationen der Erde, 4e. Aufl.
Trier, Universität, 1987.

[8] Landsberg, H.E. (Ed.)
World survey of Climatology, 16 Vols.
Elsevier, Amsterdam, 1969-1986

[9] K.N.M.I.
Climatological data of stations in The Netherlands
Normals and standard deviations for the period 1951-1980, 2nd ed.
KNMI publication 150-10, De Bilt, 1983.

[10] Mearns, L.O.; Schneider, S.H.; Thompson, S.L. and McDaniel, L.R.
Analysis of climate variability in General Circulation Models: comparison with observations and changes in variability in $2xCO_2$ experiments
Journal of Geophysical Research, 95, D12, 20,469-20,490, 1990.

[11] Katz, R.W.
Statistical procedures for making inferences about climate variability
Journal of Climate, 1, 1057-1064, 1988.

[12] Mosteller, F. and Tukey, J.W.
Data Analysis and Regression
Addison-Wesley publishing company, Reading, 1977.

[13] Box, G.E.P. and Jenkins, G.M.
Time Series Analysis forecasting and control
Holden-Day, San Francisco, 1970.

[14] Reed, D.N.
Simulation of time series of temperature and precipitation over Eastern England by an Atmospheric General Circulation Model.
Journal of Climatology, 6, 233-253, 1986.

[15] Buishand, T.A.
De variantie van de gebiedsneerslag als functie van puntneerslagen en hun onderlinge samenhang
Mededelingen Landbouwhogeschool Wageningen 77-10
Landbouwhogeschool Wageningen, Nederland, 1977.

[16] van Mourik, B.
K.N.M.I. personal communication, 1992.

[17] Chandler, T.J. and Gregory, S.
The climate of the British Isles
Longman, London, 1976.

[18] van Engelen, A.
Maandsommen der globale straling te De Bilt over het tijdvak 1961-1980
Internal note KNMI (unpublished), 1990.

[19] World Meteorological Organization
Technical Note No. 61
Note on the standardization of pressure reduction methods in the international network of synoptic stations (WMO publication 154)
World Meteorological Organization, Geneva, Switzerland, 1964.

[20] U.S. Department of commerce
World weather records 1971-1980, Vol. 2, Europe
U.S. Department of commerce, 1987.

[21] Troen, I. and Petersen, E.L.
European wind atlas
Commission of the European Communities,
Risø National Laboratory, Roskilde, Denmark, 1989.

[22] Wieringa, J.
Roughness-dependent geographical interpolation of surface wind speed averages
Quarterly Journal of the Royal Meteorological Society, **112**, 867-889, 1986.

[23] Wieringa, J. and Rijkoort, P.J.
Windklimaat van Nederland
Staatsuitgeverij, Den Haag, 1983.

[24] Houghton, J.T.; Jenkins, G.J. and Ephraums, J.J. (Eds.)
Climate Change
The IPCC Scientific Assessment
Cambridge university press, Cambridge, 1990.

[25] Katz, R.W.
Statistical evaluation of climate experiments with General Circulation Models: A parametric time series modeling approach.
Journal of the Atmospheric Sciences, **39**, 1446-1455, 1982.

[26] Davis, W.W.
Robust interval estimation of the innovation variance of an ARMA model.
The Annals of Statistics, **5**, 700-708, 1977.